

# COMPACT DUAL-BAND BANDPASS FILTER BASED ON STUB-LOADED RECTANGULAR LOOP STEPPED IMPEDANCE RESONATOR

Salif Nabouna Dembele<sup>1</sup>, Ting Zhang<sup>1</sup>, Jingfu Bao<sup>1</sup>, Denis Bukuru<sup>1</sup>, and Muhammad Ammar Khan<sup>1</sup>

<sup>1</sup>School of Electronic Science and Engineering, University of Electronic Science and Technology of China, Chengdu, 611731, China

## ABSTRACT

*This work presents a compact dual-band bandpass filter (BPF) based on stub-loaded rectangular loop stepped impedance resonator (SLRLSIR). The proposed SLRLSIR consists of two outer open-circuited and two inner open-circuited stubs, which are designed to the central sides of the rectangular loop resonator. Owing to its symmetry, even-and odd-mode analysis methods are applied to deduce the equivalent-circuit equations and to justify the structural design. The second passband can be easily tuned by changing the two inner open-circuited stubs when the first passband is fixed at a desirable frequency. The upper stopband is improved by a pair of additional open-circuited stubs stepped impedance resonators at the I/O ports. Transmission zeros are generated between passbands and stopbands. A SLRLSIR prototype dual-band BPF with central frequencies of 2.42/4 GHz is fabricated and systematically studied. The measurement results agreed well with the simulation results.*

## KEYWORDS

*Bandpass filter (BPF), Bended microstrip feed line (BMFL), Dual-band, Stub-loaded rectangular loop stepped impedance resonator (SLRLSIR), Transmission zero (TZ)*

## 1. INTRODUCTION

The recent development of modern wireless communication systems require high performance and compact multi-band bandpass filters which can reduce the number of components in RF communication systems. Therefore, dual-band bandpass filter has become an interesting and attractive research field. To meet these requirements, a large variety of dual-band/multi-band BPF has been investigated and reported [1-35].

Based on a single quadruple-mode circular ring resonator, a dual-band microstrip bandpass filter with multiple controllable transmission zeros has been investigated and implemented [1]. But, this filter suffers from poor selectivity between the two passbands. Dual-band/multiband BPFs can be achieved by combining two or more resonators using the common impedance matching circuit at the input and output ports [2-14].

By using a cascade connection of bandstop filter and wide-band BPF, dual-band BPF has been implemented and reported in [15]. However, using these methods to implement dual-band/multi-band BPFs, have a disadvantage of large circuit size. To overcome this disadvantage, various methods have been used and reported [16-24]. In [16-21], double-spiral resonators, embedded spiral resonator, complementary split-ring resonators with closely spaced passbands, split ring scheme, stepped impedance resonator and defected ground structure, and folded uniform impedance resonator have been used to miniaturize microstrip dual-band BPF for WLAN application. Capacitance loaded square loop resonator, open stub-loaded stepped impedance resonator with cross-slots, and square loop resonator have been used to implement dual-band BPF as reported in [22-24].

Moreover, in [25-31], multi-band BPFs, such as tri-, quad-, quint-, and sext-bands have been also reported. All the aforementioned works have the main objectives of reducing the circuit size and achieving high performances. However, nowadays these kinds of challenges are still existing in microwave passive circuit designs. Therefore, stub-loaded rectangular loop stepped impedance resonator (SLRLSIR) is proposed to be investigated for application in the design of compact dual-band BPF.

In this paper, a stub-loaded rectangular loop stepped impedance resonator is investigated and presented for dual-band BPF. The presented dual-band BPF operates at 2.42 GHz and 4 GHz with fractional bandwidths (BWs) of 11.57 % and 12 %, respectively. The paper is organized in the following. In section 2, the symmetric characteristics, the design equations, the coupling coefficients and the external quality factors of the proposed resonator are studied. Tuning of the position of the transmission zeros and the fractional BWs using the physical dimensions of SLRLSIR are also given. In section 3, experimental results, discussion and comparison with other reported works are given. Finally, the conclusion is given in section 4.

## 2. DESIGN PROCEDURE

The following sub-sections describe the design procedure.

### 2.1. ANALYSIS OF THE PROPOSED RESONATOR

Figure 1 shows the basic configuration of the proposed resonator. It consists of two outer open-circuited and two inner open-circuited stubs which are added to the central sides of the rectangular loop resonator.

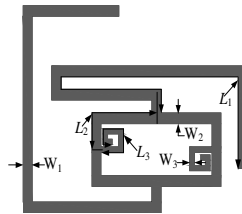


Figure 1. The proposed resonator

Based on Figure 1, the even-and odd-mode equivalent transmission-line models are depicted in Figure 2 (a) and (b), respectively.

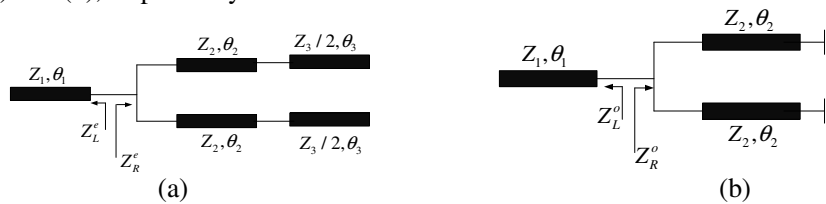


Figure 2. Equivalent transmission-line models (a) Even-mode equivalent circuit (b) Odd-mode equivalent circuit

The resonant frequencies using even-and odd-mode excitations are deduced as [1]:

$$Z_L^e + Z_R^e = 0 \tag{1}$$

$$Z_L^o + Z_R^o = 0 \tag{2}$$

where

$$Z_L^e = -jZ_1 \cot \theta_1 \quad (3)$$

$$Z_R^e = jZ_2 \frac{2Z_2 \tan \theta_2 - Z_3 \cot \theta_3}{2Z_2 + Z_3 \cot \theta_3 \tan \theta_2} \quad (4)$$

$$Z_L^o = -jZ_1 \cot \theta_1 \quad (5)$$

$$Z_R^o = j \frac{Z_2}{2} \tan \theta_2 \quad (6)$$

According to Fig. 1, the even-and odd-mode resonant frequencies  $f_{even}$  and  $f_{odd}$  of the proposed resonator are functions of the line lengths  $L_e$  and  $L_o$ , respectively, which can be expressed as:

$$f_{even} = \frac{c}{(2(L_e)\sqrt{\epsilon_{eff}})} \quad (7)$$

$$f_{odd} = \frac{c}{(4(L_o)\sqrt{\epsilon_{eff}})} \quad (8)$$

where

$$L_e = L_1 + 2L_2 + L_3 \quad (9)$$

$$L_o = L_1 + 2L_2 \quad (10)$$

$c$  is the light speed in free space and  $\epsilon_{eff}$  is the effective dielectric constant of the relative dielectric constant of the substrate.

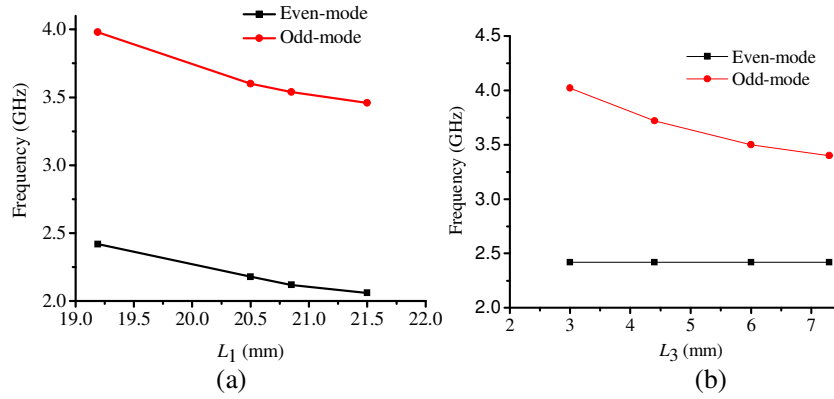


Figure 3. (a) Variation of even-and odd-mode resonant frequencies on parameter  $L_1$ , (b) Variation of even-and odd-mode resonant frequencies on parameter  $L_3$

As seen in figure 3 (a), the even-and odd-mode resonant frequencies are functions of parameter  $L_1$ . Both even-and odd-mode resonant frequencies are decreased when the parameter  $L_1$  is increased. As depicted in Figure 3 (b), the odd-mode resonant frequency is decreased when the parameter  $L_3$  is increased whereas the even-mode resonant frequency keeps constant. It means that only the odd-mode resonant frequency can be affected by varying the value of  $L_3$ .

Figure 4 shows the frequency response of the proposed resonator under weak coupling. The even-mode and odd-mode are splitting into two modes. It can be concluded that the proposed SLRLSIR is a dual-mode resonator.

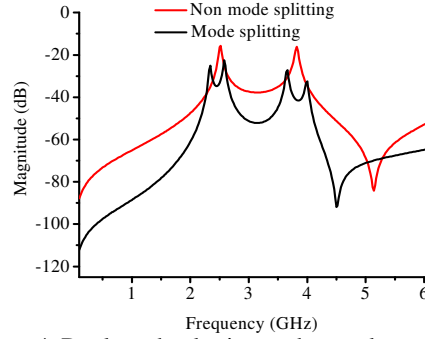


Figure 4. Dual-mode plotting under weak coupling

## 2.2. DESIGN OF DUAL-BAND BPF

Figure 5 indicates the layout of the proposed dual-band BPF. By cascading two SLRLSIRs, a second degree dual-band BPF is achieved. The two cascaded resonators are then coupled with the bended microstrip feed lines (BMFLs).

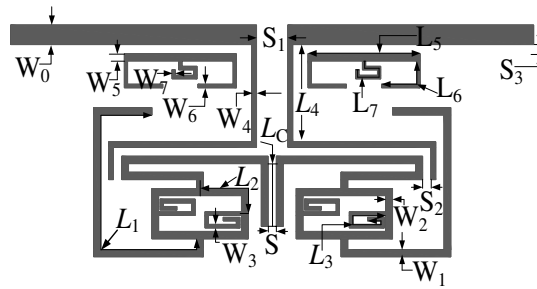


Figure 5. The layout of the proposed dual-band BPF

The coupling and routing scheme of the proposed dual-band BPF are depicted in figure 6 in which the resonators 1 and 2 are indicated by the black circles 1 and 2, respectively. The circles S and L indicate source and load, respectively, which are normalized to unity ( $g_s=g_L=g_0=1$ ).  $M_{12}$  indicates the coupling coefficient between the two resonators, while  $M_{SL}$  indicates the cross-coupling between source and load.

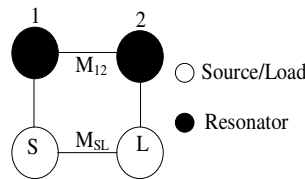


Figure 6. The coupling scheme of the proposed dual-band BPF

The proposed dual-band BPF is designed based on approximate synthesis formulas [32-34] of the standard Chebyshev low-pass prototype filter. The elements are defined as:  $g_0 = 1$ ,  $g_1 = 0.9502$ ,  $g_2 = 2.0841$ ,  $J_1 = -0.4511$ , and  $J_2 = 1.8213$ . According to the relationship between the bandpass design parameters and the standard Chebyshev low-pass prototype filter elements [32], the coupling matrices  $M_{ij}^{f_1}$  and  $M_{ij}^{f_2}$  of the proposed dual-band BPF are deduced as:

$$M_{ij}^{f_1} = \begin{bmatrix} M_{SS} & M_{S1} & M_{S2} & M_{SL} \\ M_{1S} & M_{11} & M_{12} & M_{1L} \\ M_{2S} & M_{21} & M_{22} & M_{2L} \\ M_{LS} & M_{L1} & M_{L2} & M_{LL} \end{bmatrix} \\
 = \begin{bmatrix} 0 & 0.0822 & 0 & -0.0549 \\ 0.0822 & 0 & 0.1011 & 0 \\ 0 & 0.1011 & 0 & 0.0822 \\ -0.0549 & 0 & 0.0822 & 0 \end{bmatrix} \text{ at 2.42 GHz} \quad (11)$$

$$M_{ij}^{f_2} = \begin{bmatrix} M_{SS} & M_{S1} & M_{S2} & M_{SL} \\ M_{1S} & M_{11} & M_{12} & M_{1L} \\ M_{2S} & M_{21} & M_{22} & M_{2L} \\ M_{LS} & M_{L1} & M_{L2} & M_{LL} \end{bmatrix} \\
 = \begin{bmatrix} 0 & 0.0853 & 0 & -0.0570 \\ 0.0853 & 0 & 0.1049 & 0 \\ 0 & 0.1049 & 0 & 0.0853 \\ -0.0570 & 0 & 0.0853 & 0 \end{bmatrix} \text{ at 4 GHz} \quad (12)$$

where  $M_{ij}$  is the coupling coefficient of  $M_{12} = FBW \cdot J_2 / g_2$ ,  $M_{SL} = FBW \cdot J_1 / g_1$ , and

$$M_{S1} = M_{2L} = FBW / \sqrt{g_1 g_2}$$

As seen in figure 7 (a), the coupling coefficients ( $M_{ij}$ ) of both two passbands are decreased when the space  $S$  between the two resonators is increased. It means that when the space coupling  $S$  is decreased, the stronger the coupling leads to mode splitting as shown in figure 7 (b). By using full-wave EM simulation software the coupling coefficient  $M_{ij}$  can be extracted using the following expression [35]:

$$M_{12} = (f_{p2}^2 - f_{p1}^2) / (f_{p1}^2 + f_{p2}^2) \quad (13)$$

where  $f_{p1}$  and  $f_{p2}$  indicate the two splitting resonant modes frequencies. The external quality factor  $Q_e$  can be expressed in the following expression [32]:

$$Q_e = f_0 / \Delta f_{-3dB} \quad (14)$$

where  $f_0$  is the resonant frequency and  $\Delta f_{-3dB}$  is a 3-dB bandwidth of the input or output resonator when it is alone externally excited. It should be noted that wider bandwidth needs a lower external quality factor  $Q_e$ .

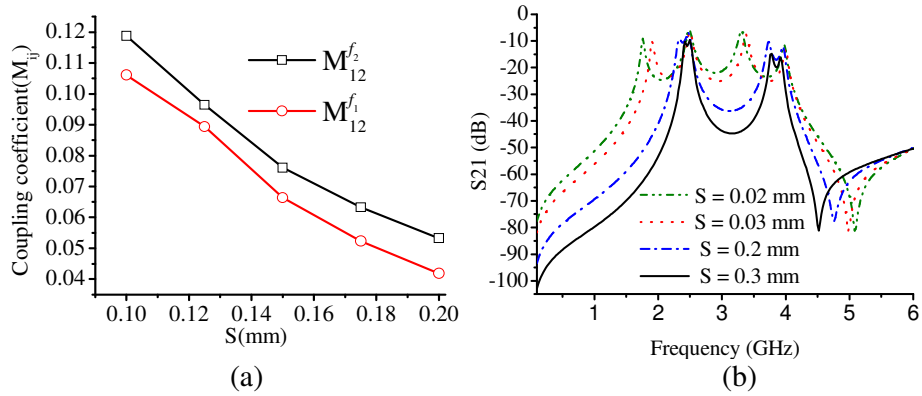


Figure 7. (a) The coupling coefficient  $M_{ij}$  with varied coupling space ( $S$ ), (b) Frequency response of  $S_{21}$  magnitudes with varied coupling space ( $S$ ) under loose coupling

In figure 8, the position of transmission zeros and the fractional bandwidths (BW)s are functions of parameter  $L_C$ . By changing  $L_C$ , the position of transmission zeros and the fractional BWs are changed as shown in figure 8. In order to obtain a desired dual-band frequency response and a suitable external quality factor  $Q_e$  for the bandwidth of both two passbands, the coupling space ( $S$ ) between the two resonators and the coupling length ( $L_C$ ) are set as:  $S = 0.1$  mm and  $L_C = 3.5$  mm, respectively. Therefore, the external quality factors  $Q_e$  of the first and second passbands are found to be 20.92 and 33.33, respectively. The second passband of the proposed dual-band BPF can easily be tuned by varying the value of  $L_3$  when the first passband is fixed at a desirable frequency (see Fig. 3).

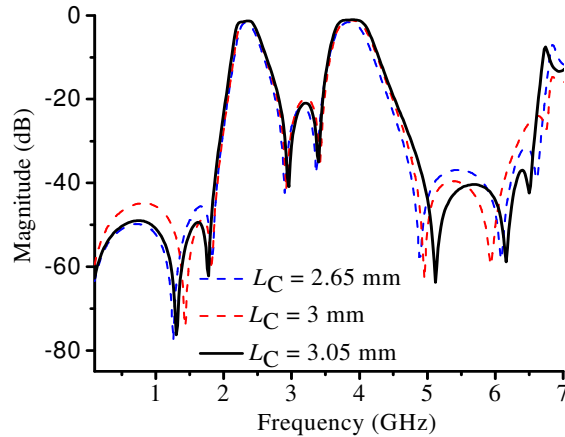
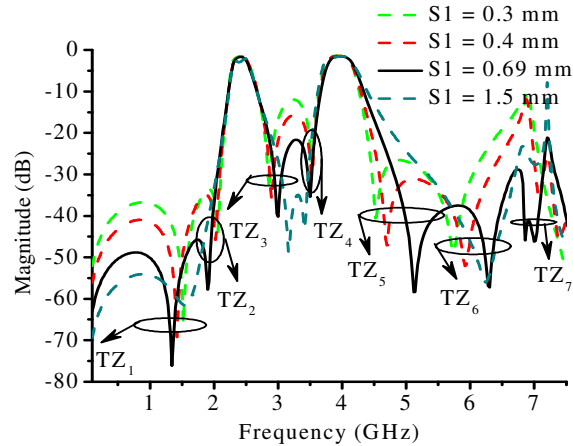


Figure 8. Variation of bandwidths on parameter  $L_C$

Based on source-load coupling method, seven transmission zeros are created as shown in Figure 9. According to the coupling matrices defined in Eq. (11) and (12), transmission zeros  $TZ_2$  and  $TZ_3$  are generated at lower and upper stopband of the first passband and transmission zeros  $TZ_4$  and  $TZ_5$  are generated at lower and upper stopband of the second passband. The transmission zeros  $TZ_1$  and  $TZ_6$  are created due to the source-load coupling method whereas transmission zero  $TZ_7$  is created due to the use of a pair of additional open-circuited stubs stepped impedance resonators at the I/O ports, which can suppress the harmonic frequency in upper stopband of the second passband. As a result, a transmission zeros can be created [24].

Figure 9. Frequency responses results with varied  $S_1$ 

### 3. EXPERIMENTAL RESULTS AND DISCUSSION

According to the above analysis, a dual-band BPF is designed and fabricated on the 0.508 mm Rogers R04350 (tm) substrate with a relative dielectric constant of 3.66 and a loss tangent of 0.004. The structure of the proposed dual-band BPF is simulated by using the HFSS software. A photograph of the fabricated dual-band BPF is shown in figure 10. The optimized physical dimensions (unit: mm) are extracted as:  $L_1 = 18.19$ ,  $L_2 = 4.9$ ,  $L_3 = 3$ ,  $L_4 = 4.78$ ,  $L_5 = 6.76$ ,  $L_6 = 3.62$ ,  $L_7 = 3.5$ ,  $L_C = 3.5$ ,  $W_0 = 1.09$ ,  $W_1 = 0.4$ ,  $W_2 = 0.4$ ,  $W_3 = 0.2$ ,  $W_4 = 0.3$ ,  $W_5 = 0.4$ ,  $W_6 = 0.2$ ,  $W_7 = 0.2$ ,  $S = 0.1$ ,  $S_1 = 0.69$ ,  $S_2 = 0.1$ ,  $S_3 = 0.1$ . The proposed dual-band BPF measures 20.3 mm  $\times$  7.89 mm. In terms of wavelength, the size can be estimated as  $0.27\lambda_g \times 0.10\lambda_g$ , where  $\lambda_g$  is the guided-wavelength at the center frequency of the lower passband.

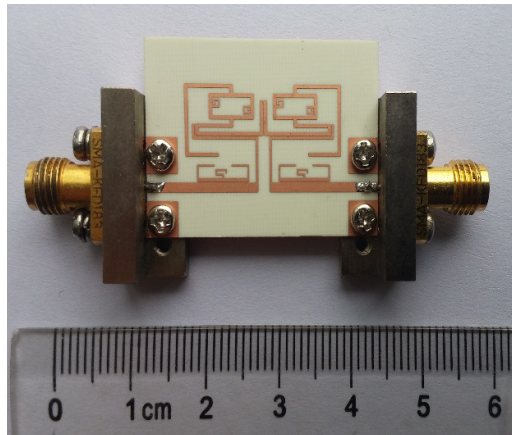


Figure 10. Photograph of the fabricated dual-band BPF

The measurement results of the proposed dual-band BPF are obtained by using Agilent R&S ZVA50 Vector Network Analyzer. Simulated and measured results are shown in figure 11. The measured results of the lower passband and upper passband are centered at 2.42/4 GHz with 3-dB fractional bandwidths of 11.57/12%, respectively. The measured and simulated minimum insertion losses of both two passbands including the loss from SMA connectors are better than 1.52/1.34 dB and 1.48/1.36 dB, respectively and the measured and simulated return losses of both two passbands are greater than 20/25 dB and 15/23 dB, respectively. The lower and upper stopband attenuations are greater than 45 dB and 30 dB, respectively. The isolation between the

two passbands is better than 22 dB. As shown in figure 11, the simulated and measured results are in good agreement. However, the measured results reveal a spurious frequency response in the upper stopband of the second passband and some slight discrepancies between the simulated and measured results might be due to the fabrication errors.

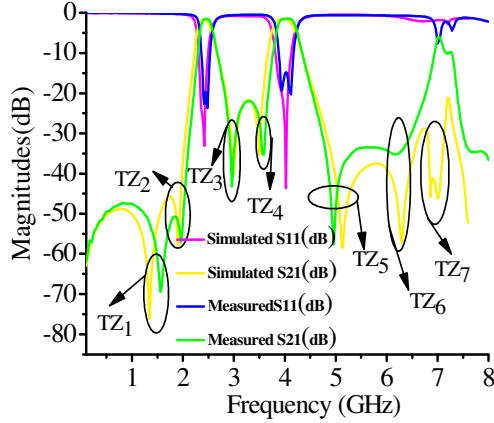


Figure 11. Simulated and Measured results of the fabricated dual-band BPF

Table 1 illustrates the performance comparison between this work and the reported works. As it can be observed in Table 1, it has demonstrated a compact size as the major contribution of this work and it also exhibits better insertion losses of both two passbands. However, it has larger insertion loss of lower passband compared with [5].

Table 1. Performance comparison with the reported works.

References	$f_1/f_2$ (GHz)	3-dB Fractional Bandwidth (%)	Insertion loss (dB)	Transmission zeros	Size ( $\lambda_g \times \lambda_g$ )
[4]	1.8/2.4	5.6/3	1.6/2.5	1	0.2×0.25
[5]	2.4/5.8	4.63/3.6	1.35/1.97	3	0.39×0.25
[6]	2.4/5.2	10.3/6.0	2.27/2.88	3	0.42×0.26
[22]	1.8/2.36	2.22/1.70	2.0/1.9	3	0.47×0.38
This work	2.42/4	11.57/12	1.52/1.48	6	0.27×0.10

#### 4. CONCLUSIONS

A compact dual-band BPF using two cascaded SLRLSIRs is presented in this paper. The proposed dual-band BPF operating at 2.42/4 GHz for wireless communication systems application is designed and fabricated. Six transmission zeros have been achieved, resulting in high frequency selectivity. Better insertion losses and compact size of  $0.27\lambda_g \times 0.10\lambda_g$  are achieved. The measured results are in good agreement with the simulated ones. The compactness in circuit size makes the proposed dual-band BPF a good candidate for wireless communication systems using multiband applications.

#### ACKNOWLEDGMENTS

This work was supported by the National Natural Science Foundation of China (Grant No.U1430102).

**REFERENCES**

- [1] Li, D., Zhang, Y., Ai, J., Song, K., & Fan, Y., (2017) "Dual-band bandpass filter with multiple controllable transmission zeros and wide stopband", *Microwave Journal*, Vol. 60, No. 6, pp1-8.
- [2] Miyake, H., Kitazawa, S., Ishizaki, T., Yamada, T., & Nagatomi, Y., (1997) "A miniaturized monolithic dual band filter using ceramic lamination technique for dual mode portable telephones", In *Microwave Symposium Digest 1997, IEEE MTT-S International*, Vol. 2, pp789-792.
- [3] Zhang, X.Y., Shi, J., Chen, J.X., & Xue, Q., (2009) "Dual-band bandpass filter design using a novel feed scheme", *IEEE Microwave and Wireless Components Letters*, Vol. 19, No. 6, pp350-352.
- [4] Hung, C.Y., Yang, R.Y., & Lin, Y.L., (2010) "A simple method to design a compact and high performance dual-band bandpass filter for GSM and WLAN", *Progress In Electromagnetics Research C*, Vol. 13, pp187-193.
- [5] Zhang, Z.C., Chu, Q.X., & Chen, F.C., (2015) "Compact dual-band bandpass filters using open-/short-circuited stub-loaded  $\lambda/4$  resonators", *IEEE Microwave and Wireless Components Letters*, Vol. 25, No. 10, pp657-659.
- [6] Kim, C.H., & Chang, K., (2011) "Independently controllable dual-band bandpass filters using asymmetric stepped-impedance resonator", *IEEE Transactions on Microwave Theory and Techniques*, Vol. 59, No. 12, pp3037-3047.
- [7] Xie, Y., Chen, F.C., & Li, Z., (2017) "Design of dual-band bandpass filter with high isolation and wide stopband", *IEEE Access*, Vol. 5, pp25602-25608.
- [8] Chen, C.Y., & Hsu, C.Y., (2006) "A simple and effective method for microstrip dual-band filters design" *IEEE Microwave and Wireless Components Letters*, Vol. 16, No. 5, pp246-248.
- [9] Zhang, X.Y., & Xue, Q., (2007) "Novel dual-mode dual-band filters using coplanar waveguide-fed ring resonators", *IEEE Transactions on Microwave Theory and Techniques*, Vol. 55, No. 10, pp2183-2190.
- [10] Weng, M.H., Huang, C.Y., Wu, H.W., Shu, K., & Su, Y.K., (2007) "Compact dual-band bandpass filter with enhanced feed coupling structures", *Microwave and Optical Technology Letters*, Vol. 49, No. 1, pp171-173.
- [11] Chen, J.X., Yum, T.Y., Li, J.L., & Xue, Q., (2006) "Dual-mode dual-band bandpass filter using stacked-loop structure", *IEEE Microwave and Wireless Components Letters*, Vol. 16, No. 9, pp502-504.
- [12] Chen, C.H., Huang, C.H., Horng, T.S., & Wu, S. M., (2012) "Highly miniaturized multiband bandpass filter design based on a stacked spiral resonator structure", *IEEE Transactions on Microwave Theory and Techniques*, Vol. 60, No. 5, pp1278-1286.
- [13] Yu, B., Jia, B., & Zhu, Z., (2015) "Compact tri-band bandpass filter with stub-loaded stepped-impedance resonator", *Electronics Letters*, Vol. 51, No. 9, pp701-703.
- [14] Liu, H., Song, Y., Ren, B., Wen, P., Guan, X.H., & Xu, H., (2017) "Balanced tri-band bandpass filter design using octo-section stepped-impedance ring resonator with open stubs", *IEEE Microwave and Wireless Components Letters*, Vol. 27, No. 10, pp912-914.
- [15] Tsai, L.C., & Hsue, C.W., (2004) "Dual-band bandpass filters using equal-length coupled-serial-shunted lines and Z-transform technique", *IEEE Transactions on Microwave Theory and Techniques*, Vol. 52, No. 4, pp1111-1117.
- [16] Wu, G.C., Wang, G., Liang, J.G., Gao, X.J., & Zhu, L., (2015) "Miniaturized microstrip dual-band bandpass filter using novel symmetric double-spiral resonators for WLAN application", *Electronics Letters*, Vol. 51, No. 15, pp1177-1178.
- [17] Luo, X., Qian, H., Ma, J.G., Ma, K., & Yeo, K.S., (2010) "Compact dual-band bandpass filter using novel embedded spiral resonator (ESR)", *IEEE Microwave and Wireless Components Letters*, Vol. 20, No. 8, pp435-437.

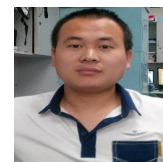
- [18] Liu, S., Xu, J., & Xu, Z.T., (2016) “ Compact dual-band bandpass filters using complementary splitting resonators with closely spaced passbands” *Electronics Letters*, Vol. 52, No. 15, pp1312-1314.
- [19] Wu, G., Yang, L., & Xu, Q., (2015) “Miniaturized dual-band filter with high selectivity using splitting scheme”, *Electronics Letters*, Vol. 51, No. 7, pp570-572.
- [20] Song, K., Zhang, F., & Fan, Y., (2014) “Miniaturized dual-band bandpass filter with good frequency selectivity using SIR and DGS”, *AEU-International Journal of Electronics and Communications*, Vol. 68, No. 5, pp384-387.
- [21] Hayati, M., Khajavi, A., & Abdi, H., (2013) “A miniaturized microstrip dual-band bandpass filter using folded UIR for multimode WLANs”, *Applied Computational Electromagnetics Society Journal*, Vol. 28, No. 1, pp35-39.
- [22] Fu, S., Wu, B., Chen, J., Sun, S.J., & Liang, C.H., (2012) “Novel second-order dual-mode dual-band filters using capacitance loaded square loop resonator”, *IEEE Transactions on Microwave Theory and Techniques*, Vol. 60, No. 3, pp477-483.
- [23] Denis, B., Song, K., & Zhang, F., (2017) “Compact dual-band bandpass filter using open stub-loaded stepped impedance resonator with cross-slots”, *International Journal of Microwave and Wireless Technologies*, Vol. 9, No. 2, pp269-274.
- [24] Deng, K., Yang, S., Sun, S.J., Wu, B., & Shi, X.W., (2013) “Dual-mode dual-band bandpass filter based on square loop resonator”, *Progress In Electromagnetics Research C*, Vol. 37, pp119-130.
- [25] Mo, Y., Song, K., & Fan, Y., (2014) “Miniaturized tri-band bandpass filter using coupled lines and grounded stepped impedance resonator”, *IEEE Microwave and Wireless Components Letters*, Vol. 24, No. 5, pp333-335.
- [26] Meesonklin, S., Chomtong, P., & Akkarakyhalin, P., (2016) “A compact multiband BPF using step-impedance resonators with interdigital capacitors”, *Radioengineering*, Vol. 25, No. 2, pp258-267.
- [27] Lan, S.W., Weng, M.H., Ye, C.S., & Hung, C.Y., (2015) “Compact quad-band bandpass filter based on uniform impedance stub-loaded resonators”, *IEEE Transactions on Microwave Theory and Techniques*, Vol. 7, No. 2, pp121-126.
- [28] Yang, Q., Jiao, Y.C., & Zhang, Z., (2018) “Compact multiband bandpass filter using low-pass filter combined with open stub-loaded shorted stub”, *IEEE Transactions on Microwave Theory and Techniques*, Vol. 66, No. 4, pp1926-1938.
- [29] Ai, J., Zhang, Y., Da Xu, K., Li, D., & Fan, Y., (2016) “Miniaturized quint-band bandpass filter based on multi-mode resonator and  $\lambda/4$  resonators with mixed electric and magnetic coupling”, *IEEE Microwave and Wireless Components Letters*, Vol. 26, No. 5, pp343-345.
- [30] Tang, J., Liu, H., Zhang, Q., Ren, B., & Liu, Y., (2018) “Miniaturized multiband HTS bandpass filter design using a single-perturbed multimode resonator with multitransmission zeros”, *IEEE Transaction on Applied Superconductivity*, Vol. 28, No. 4, pp1-5.
- [31] Ai, J., Zhang, Y., Da Xu, K., Guo, Y., Joines, W.T., & Liu, Q.H., (2016) “Compact sext-band bandpass filter based on single multimode resonator with high band-to-band isolation”, *Electronics Letters*, Vol. 52, No. 9, pp729-731.
- [32] Hong, J.S., & Lancaster, M. J., (2000) “Design of high selective microstrip bandpass filters with a single pair of attenuation poles at finite frequencies”, *IEEE Transactions on Microwave Theory and Techniques*, Vol. 48, No. 7, pp1098-1107.
- [33] Crnojevic-Bengin, V., (2015) *Advances in multi-band microstrip filters*, Cambridge University Press.
- [34] Hong, J.S.G., & Lancaster, M.J., (2004) *Microstrip filters for RF/microwave Applications*, John Wiley & Sons.
- [35] Hong, J.S., & Lancaster, M.J., (1996) “ Couplings of microstrip square open-loop resonators for cross-coupled planar microwave filters”, *IEEE Transactions on Microwave Theory and Techniques*, Vol.44,No.11,pp2099-2109.

## AUTHORS

**Salif Nabouna Dembele** received the M.S. degree in physical electronics from the University of Electronic Science and Technology of China (UESTC) in June 2015 and is now pursuing his Ph.D. degree in electromagnetic field and microwave technology at the University of Electronic Science and Technology of China (UESTC), Chengdu, China, from September 2015. His research interests include microwave passive components design, RF MEMS technology, and circuits and systems.



**Ting Zhang** received the M.S. degree in electronics and communication engineering from the University of Electronic Science and Technology of China (UESTC) in 2015 and is now pursuing his Ph.D. degree in circuit and system at the University of Electronic Science and Technology of China (UESTC), Chengdu, China from 2015. His research interests include microwave planar multiplexer, filter, oscillator, RF MEMS switch, tunable filter and microwave circuit.



**Jingfu Bao** was born in Zhejiang, China in 1964. He received his BSc, MSc, and PhD degrees from UESTC, Chengdu, in 1986, 1989, and 1996, respectively, all in electronic engineering. In 1998, he was with SONY, Japan, where he worked on wireless RF circuit research until 2004. Since 2004, he has been with the School of Electronic Engineering, UESTC. Currently, he is a professor with the School of Electronic Science and Engineering, UESTC. His research interests include MEMS technology, frequency synthesis, and high-frequency power amplifying device.



**Denis Bukuru** received the M.S. degree in electromagnetic field and microwave technology from the University of Electronic Science and Technology of China (UESTC) in 2013, and Ph.D. degree in electromagnetic field and microwave technology at the University of Electronic Science and Technology of China (UESTC), Chengdu, China, from 2017. His research interests include microwave/millimeter-wave devices, circuits, and systems.



**Muhammad Ammar Khan** received his Doctor degree in 2015 from UESTC Chengdu in the field of Engineering Physics. Currently he is working as Senior Research Fellow in School of Electronic Science Engineering, UESTC. His research interests include Polymers, Diodes, Organic Semiconductors, Electrical properties of Materials, Radio frequency devices, MEMS technology.

